

A joint theoretical and experimental investigation on the ^{13}C and ^1H NMR chemical shifts of coumarin derivatives

Philippe d'Antuono · Edith Botek ·
Benoît Champagne · Laetitia Maton ·
Dorothee Taziaux · Jean-Louis Habib-Jiwan

Received: 17 May 2009 / Accepted: 5 August 2009 / Published online: 28 August 2009
© Springer-Verlag 2009

Abstract ^1H and ^{13}C NMR chemical shifts of coumarin derivatives have been determined using first principles approaches with and without accounting for the effects of the solvent and compared to experiment in order to assess their reliability. Good linear relationships are obtained between theory and experiment, which allows correcting the calculated values for systematic errors. This is particularly the case when using the PCM scheme to model the solvent effects because the δ values larger than 150 ppm are more difficult to reproduce. The final accuracy of the method amounts to about 1 ppm for ^{13}C and 0.05 ppm for ^1H .

Keywords Chemical shift · Coumarin derivatives · Coupled-perturbed Kohn-Sham · Solvent effects on the chemical shift · Conformation impact and Maxwell–Boltzmann averaging

Dedicated to Professor Sandor Suhai on the occasion of his 65th birthday and published as part of the Suhai Festschrift Issue.

P. d'Antuono · E. Botek · B. Champagne (✉)
Laboratoire de Chimie Théorique Appliquée,
Facultés Universitaires Notre-Dame de la Paix (FUNDP),
rue de Bruxelles, 61, 5000 Namur, Belgium
e-mail: benoit.champagne@fundp.ac.be

L. Maton · D. Taziaux · J.-L. Habib-Jiwan
Unité de Chimie des Matériaux Organiques et Inorganiques,
Université Catholique de Louvain, Place Louis Pasteur, 1,
1348 Louvain-la-Neuve, Belgium

Present Address:

P. d'Antuono
Institut des Sciences Moléculaires, UMR 5255 CNRS,
Université de Bordeaux, Cours de la Libération, 351,
33405 Talence Cedex, France

1 Introduction

Ab initio calculations have become valuable tools to help in interpreting NMR spectra as well as in deducing from these spectra information on the electronic structure of molecules [1–5] and polymers [6, 7]. In particular, density functional theory (DFT) schemes offer a good compromise between computational cost and reliability and therefore present the potential to assist in assigning experimental spectra. Indeed, the errors on the chemical shifts are often systematic in nature and they can be corrected using linear scaling procedures [8–10]. In the case of ^1H chemical shifts, Rablen et al. [9] determined the linear scaling parameters for a collection of exchange-correlation (XC) functionals combined with different atomic basis sets and found that the root-mean-square error on the so-predicted chemical shifts in comparison with solution experimental values can be as small as 0.15 ppm. More recent investigations on Cl containing systems and PVC chains have confirmed this high performance, at least, as far as distinction is made between chemically different atoms [7, 10]. So, DFT has been broadly employed for simulating NMR spectra [9–26]. Among these, DFT calculations helped in (1) determining the configuration of passifloricin A [11], (2) re-interpreting the ^1H NMR spectra of the *E* and *Z* isomers of alkyl phenyl ketone phenylhydrazones [12], and (3) in reassigning the structure of hexacyclinol to a diepoxide [22]. On the other hand, substantial methodological efforts have been made to estimate chemical shifts with high accuracy, accounting therefore for electron correlation, solvent, ro-vibrational, and temperature effects [1–5]. Nevertheless, such schemes are still nowadays restricted to rather small compounds.

In the course of the investigations on fluoroionophores by some of us [27–30], we have initiated a joint experimental–

theoretical collaboration aiming first at interpreting NMR spectra. Our interest in fluoroionophores finds its origin in their ability to highlight selectively the complexation of ions via a modification of their photophysical properties [31, 32] and in their performance to detect a large range of analytes such as alkaline and alkalino-earth cations, heavy and transition metals, protons, and anions. Like for photochromic compounds [33–35], in addition to the characterization of their optical properties, fluoroionophores are often subjected to the detailed NMR characterization.

In particular, fluoroionophores based on the coumarin-343 (C343) fluorescent unit are the subject of intense investigation. In this paper, we first assess the performance of DFT methods and atomic basis sets to predict the ^1H and ^{13}C NMR chemical shifts of coumarin derivatives (Fig. 1) by comparing theoretical values to experiment. In particular, this assessment extends our previous investigations dealing with PVC segments to aromatic systems. For reasons described above, this validation step is carried out by comparison with experiment rather than with results obtained using highly elaborated methods and it results in linear regressions equations that will be used when investigating other compounds.

In the second step, the efficiency of this approach is exemplified (Fig. 1) on coumarin-343 diethylamide (C343-

dea, **3**), coumarin-343-crown (C343-crown, **4**), and coumarin-343-dibenzocrown (C343-dibenzocrown, **5**). The paper is organized as follows. The experimental aspects are described in Sect. 2 while Sect. 3 presents the computational procedure. Then, the results are given and analyzed in Sect. 4 before conclusions are drawn in Sect. 5.

2 Experimental aspects

The syntheses of C343-dea [30], C343-crown [27], and C343-dibenzocrown [29] have already been described. Additional NMR spectra were recorded at a temperature of 20.0 ± 0.1 °C in deuterated acetonitrile on a BRUKER Avance 500 spectrometer installed at UCL. The concentrations of solutions were 10^{-2} M for the ^{13}C NMR spectra and 10^{-3} M for the ^1H NMR spectra. Larger concentrations were employed for ^{13}C NMR because it is less sensitive than ^1H NMR. 2D ^1H - ^1H and ^1H - ^{13}C NMR spectra were also recorded to attribute the peaks.

3 Computational procedure

Ground state molecular geometries were determined at the DFT level using the hybrid B3LYP exchange-correlation

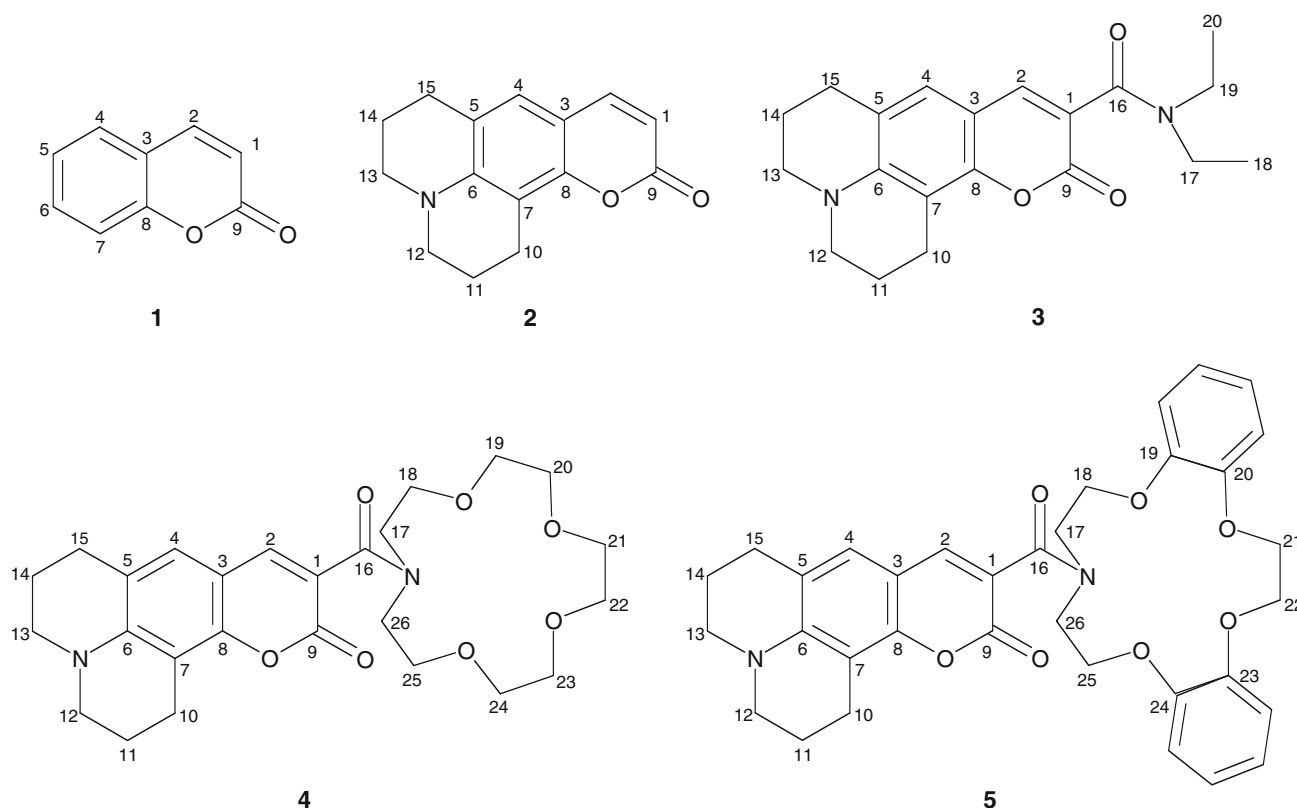


Fig. 1 Sketch of coumarin (**1**), coumarin-6H (**2**), coumarin-343 diethylamide (**3**), coumarin-343-crown (**4**), coumarin-343-dibenzocrown (**5**). The backbone atom numbering is provided to help defining the torsion angles

(XC) functional and the 6-311G(*d*) basis set with a tight convergence threshold on the residual forces on the atoms of 1.5×10^{-5} Hartree/Bohr or Hartree/radian. The NMR chemical shifts (δ_A , $A = {}^{13}\text{C}$ or ${}^1\text{H}$) were calculated as the differences of isotropic shielding constants (σ) with respect to the TMS reference ($\delta_A = \sigma_{\text{TMS}} - \sigma_A$). To reduce the systematic method-related errors, the same method was employed for both the coumarin-based compounds and TMS, for the geometry optimization as well as for the evaluation of the shielding tensor. These tensor elements and chemical shifts were evaluated adopting the coupled-perturbed Kohn-Sham procedure together with the GIAO [36, 37] approach to ensure origin-independence. Such procedure was employed using the HF approach, DFT with the B3LYP and *mPW1PW91* exchange-correlation (XC) functionals as well as at the Møller-Plesset second-order perturbation theory level (MP2). The choice of these two hybrid XC functionals is dictated by their usually good performance while it is interesting to study the impact of different percentages of HF exchange (20% for B3LYP and 25% for *mPW1PW91*). The following list of rather extended atomic basis sets was used: 6-311+G(2*d,p*), cc-pVDZ, cc-pVTZ, aug-cc-pVDZ, and aug-cc-pVTZ. To account for solvent (acetonitrile) effects, the standard Polarizable Continuum Model (PCM) [38–40] was employed within the Integral Equation Formalism (IEF). Moreover, when a molecule can adopt several stable conformations, their relative populations at a specific temperature have been determined using the Maxwell–Boltzmann (MB) distribution scheme and the reported chemical shifts are average quantities considering the so-called populations. All calculations were performed using the Gaussian 03 program [41].

4 Results and discussion

4.1 Geometrical structures

In their ground state, coumarin presents a single stable conformation whereas there are two for coumarin-6H, seven for C343-dea, six for C343-crown, and just one for the less flexible C343-dibenzocrown. The important torsion angles are listed in Table 1.

For coumarin-6H, the two non-aromatic six-membered rings of both conformers display a pseudo-chair conformation while their relative positions with respect to the mean molecular plane are inverted between the two conformers. At 298.15 K, their corresponding populations according to the MB scheme are in the 68:32 ratio for gas phase while 58:42 when considering the solvent effects using the PCM model. For C343-dea, the conformers differ by the orientations of the amide function and of the flexible ethyl branches on the N atom. As a consequence, several

conformers present very similar energies and are influenced by the PCM treatment of the solvent effects. Indeed, the relative populations of conformers **a–g** goes from 21:21:20:19:8:8:3 without solvent to 15:13:16:14:16:17:9 upon including solvent effects. The conformers come in pairs, except for compound **g**. Structures **a–b** and **c–d** differ only by the position of one of the ethyl branches of the claw, while conformers **e–f** are symmetric with respect to the plane of the molecule. For C343-crown, six conformers contribute to the MB distribution at 298.15 K and they differ by the relative position of the crown moiety as well as of the amide CO group with respect to the plane of the coumarin moiety. The relative populations of conformers **a–f** are in the 61:24:8:5:1:1 ratio without solvent (47:27:9:6:6:5 with solvent effects). For compound **5**, there is only one stable conformer as a result of the rigidification of the crown moiety by the two phenyl rings.

4.2 ${}^{13}\text{C}$ chemical shifts

The theoretical values of ${}^{13}\text{C}$ δ of compounds **1** and **2** obtained using different methods described in the previous section are listed in Table 2 and are compared to the experimental values recorded for solutions in acetonitrile. Except for a few values obtained at the MP2 level, if the solvent effects are not taken into account, the theoretical predictions overestimate the experimental ${}^{13}\text{C}$ δ values. Moreover, the differences between theory and experiment do not present a completely systematic trend and therefore, none of these methods can be concluded being much superior to the others. In particular, contrary to Cl-containing molecules [10], the largest overestimations are not necessarily associated with the largest chemical shifts, even if the trend is globally followed. When going from coumarin to coumarin-6H, these trends remain for analogous C atoms whereas some δ values can change by up to 10–15 ppm as a result of steric and electronic effects of the additional rings.

Although some of the differences between calculations and experiment are partly not systematic, the linear regressions are characterized by rather large correlation coefficients ($R > 0.99$). In fact, two approaches were adopted in these linear fits. First, all C atoms were considered in the fit; second, only the sp^2 C atoms. In this way, distinction is made between aromatic and non-aromatic C atoms while distinctions were made between C atoms bearing different numbers of Cl atoms in Ref. [10]. The respective parameters are listed in Table 3 for the different levels of approximation. Since with both XC functionals, the slope (b) is close to one and the intercept at the origin (a) is negative, in average, the overestimation of the sp^2 ${}^{13}\text{C}$ chemical shifts is a constant amounting to about 4 ppm. On the other hand, at the HF level, the intercept is positive

Table 1 Relative conformer energies (without zero-point corrections, kJ/mol), MB population ratios (in parentheses), and selected torsion angles θ (in degrees) for coumarin-6H, C343-dea, C343-crown, and C343-dibenzocrown as determined at the PCM/B3LYP/6-311G(*d*) level of approximation

Conformers	Coumarin-6H					
	ΔE (%)	$\theta_{4-5-15-14}$	$\theta_{5-15-14-13}$	$\theta_{5-6-N-13}$	$\theta_{8-7-10-11}$	$\theta_{7-10-11-12}$
a	0.0 (58)	−157.3	−49.7	11.5	160.4	46.7
b	0.8 (42)	146.4	56.5	7.5	150.8	53.6
	C343-dea					
	ΔE (%)	$\theta_{2-1-16-N}$	$\theta_{1-16-N-17}$	$\theta_{16-N-17-18}$	$\theta_{1-16-N-19}$	$\theta_{16-N-19-20}$
a	0.2 (15)	−138.1	179.9	−81.3	14.6	−122.7
b	0.6 (13)	−138.9	−179.7	79.8	14.9	−125.7
c	0.2 (16)	137.1	−14.6	123.0	−179.7	81.7
d	0.4 (14)	137.8	179.5	−80.2	−15.0	125.9
e	0.1 (16)	−133.6	−177.8	86.3	9.7	89.1
f	0.0 (17)	133.2	178.2	−87.1	−9.1	−88.2
g	1.6 (9)	133.6	−6.1	−124.1	169.9	81.4
	C343-crown					
	ΔE (%)	$\theta_{2-1-16-N}$	$\theta_{1-16-N-17}$	$\theta_{16-N-17-18}$	$\theta_{1-16-N-26}$	$\theta_{16-N-26-25}$
a	0.0 (47)	81.7	178.1	74.5	7.8	−110.8
b	1.4 (27)	124.4	169.7	75.8	−0.1	−123.6
c	4.2 (9)	−138.2	179.1	75.8	15.9	−123.7
d	5.0 (6)	−130.9	4.7	110.0	−170.2	−78.5
e	5.1 (6)	−136.4	176.4	81.6	12.6	−123.6
f	5.8 (5)	−68.7	−23.6	120.8	172.9	−68.4
	C343-dibenzocrown					
	ΔE (%)	$\theta_{2-1-16-N}$	$\theta_{1-16-N-17}$	$\theta_{16-N-17-18}$	$\theta_{1-16-N-26}$	$\theta_{16-N-26-25}$
a	0.0 (100)	−142.0	177.8	74.3	20.3	−127.3

while the slope is much smaller than unity, illustrating the impact of the lack of electron correlation. When considering all C atoms, the conclusions are partly different because for the sp^3 ^{13}C atoms theory underestimates the variation of δ values ($b < 1$). Representing the relationship between experimental and theoretical results (Fig. 2) further shows that theory is misleading in estimating the δ values for the most deshielded sp^2 C atoms. In addition, as seen from the coumarin-6H results, the MP2 estimates are poorer than the DFT values because the errors are much less systematic, leading to inversions in the relative amplitudes of the chemical shifts. This cannot be related to an approximate MB distribution because there is only one stable conformer for this compound. In terms of atomic basis set choice, the performance of the 6-311+G(2*d*,*p*) basis set is not improved when using the sequence of cc-pVXZ and aug-cc-pVXZ basis sets ($X = \text{D, T}$). Using the linear regression parameters, the B3LYP/6-311+G(2*d*,*p*) approach leads to a corrected mean absolute error (CMAE) of 1.49 and 1.63 ppm with Eqs. 1 and 2, respectively, in comparison

with 4.41 and 4.78 ppm when no correction is performed. Smaller CMAE values (1.45 and 1.52 ppm) characterize the use of the *m*PW1PW91 XC functional whereas the HF method presents larger CMAEs (2.53 and 2.36 ppm).

Looking for improving these estimates (and MAEs), solvent effects were considered in the evaluation of the chemical shifts (Tables 2, 3; Fig. 2) while using the geometries optimized without solvent effects. Indeed, additional geometry optimizations with the PCM scheme have shown that the geometrical changes are negligible, as are the corresponding changes in the MB distributions.

With respect to the calculations in gas phase, one observes that: (1) the DFT as well as the MP2 approaches still overestimate experiment systematically, (2) the *R* coefficients at the DFT level increase slightly, getting even closer to one, (3) considering the sp^2 C atoms, the slopes get smaller than one by as much as 6–7% while the intercepts reduce to about 2 ppm at the DFT level, (4) MP2 results for coumarin are of similar accuracy to those calculated using DFT, and (5) although the MAE values get

Table 2 Theoretical [HF, B3LYP, *m*PW1PW91, and MP2 methods using the 6-311+G(2*d*,*p*) basis set] and experimental (in acetonitrile) ¹³C chemical shifts (in ppm) for coumarin and coumarin-6H

Atoms	Theory, in vacuo				Theory, in acetonitrile (PCM)				Experiment
	HF	B3LYP	<i>m</i> PW1PW91	MP2	HF	B3LYP	<i>m</i> PW1PW91	MP2	
Coumarin									
C ₁	118.22 (1.01)	122.54 (5.33)	122.15 (4.94)	121.27 (4.06)	114.88 (−2.33)	120.87 (3.66)	120.57 (3.36)	121.07 (3.86)	117.21
C ₂	153.71 (9.23)	149.01 (4.53)	148.47 (3.99)	141.35 (−3.13)	160.91 (16.43)	154.74 (10.26)	154.14 (9.66)	147.39 (2.91)	144.48
C ₃	121.75 (1.94)	125.71 (5.90)	124.02 (4.21)	124.08 (4.27)	122.19 (2.38)	126.48 (6.67)	124.69 (4.88)	126.17 (6.36)	119.81
C ₄	135.98 (6.86)	132.81 (3.69)	132.39 (3.27)	126.15 (−2.97)	138.74 (9.62)	135.33 (6.21)	134.90 (5.78)	130.23 (1.11)	129.12
C ₅	126.16 (0.90)	128.05 (2.79)	127.35 (2.09)	126.54 (1.28)	128.27 (3.01)	130.72 (5.46)	130.06 (4.80)	131.51 (6.25)	125.26
C ₆	141.50 (8.92)	137.20 (4.62)	136.74 (4.16)	129.76 (−2.82)	143.83 (11.25)	139.60 (7.02)	139.20 (6.62)	132.57 (−0.01)	132.58
C ₇	121.91 (4.58)	122.10 (4.77)	121.56 (4.23)	121.05 (3.72)	121.46 (4.13)	122.41 (5.08)	121.89 (4.56)	121.97 (4.64)	117.33
C ₈	164.67 (9.85)	164.54 (9.72)	162.86 (8.04)	159.84 (5.02)	164.19 (9.37)	164.01 (9.19)	162.30 (7.48)	159.74 (4.92)	154.82
C ₉	166.65 (5.41)	163.46 (2.22)	162.29 (1.05)	158.86 (−2.38)	172.03 (10.79)	168.12 (6.88)	166.82 (5.58)	165.77 (4.53)	161.24
Coumarin-6H									
C ₁	114.27 (5.29)	114.00 (5.02)	113.66 (4.68)		105.24 (−3.74)	110.60 (1.62)	110.44 (1.46)		108.98
C ₂	157.00 (11.37)	148.16 (2.53)	147.95 (2.32)		163.66 (18.03)	152.97 (7.34)	152.81 (7.18)		145.63
C ₃	114.16 (4.90)	115.83 (6.57)	114.09 (4.83)		108.00 (−1.26)	115.80 (6.54)	113.93 (4.67)		109.26
C ₄	138.15 (11.62)	131.87 (5.34)	131.29 (4.76)		138.97 (12.44)	133.09 (6.56)	132.56 (6.03)		126.53
C ₅	122.29 (2.50)	122.08 (2.29)	120.47 (0.68)		120.52 (0.73)	126.20 (6.41)	124.52 (4.73)		119.79
C ₆	159.64 (12.27)	151.78 (4.41)	150.59 (3.22)		161.31 (13.94)	153.54 (6.17)	152.83 (5.46)		147.37
C ₇	114.12 (6.66)	113.09 (5.63)	111.59 (4.13)		109.09 (1.63)	113.40 (5.94)	111.84 (4.38)		107.46
C ₈	166.44 (13.37)	162.32 (9.25)	160.74 (7.67)		163.42 (10.35)	161.38 (8.31)	159.78 (6.71)		153.07
C ₉	170.16 (7.01)	164.54 (1.39)	163.34 (0.19)		173.46 (10.31)	169.17 (6.02)	167.80 (4.65)		163.15
C ₁₀	24.42 (1.87)	24.40 (1.85)	23.12 (0.57)		19.92 (−2.63)	24.52 (1.97)	23.22 (0.67)		22.55
C ₁₁	26.30 (4.63)	25.19 (3.52)	23.51 (1.84)		22.02 (0.35)	24.81 (3.14)	23.13 (1.46)		21.67
C ₁₂	51.82 (0.87)	53.60 (2.65)	51.89 (0.94)		46.33 (−4.62)	53.29 (2.34)	51.61 (0.66)		50.95
C ₁₃	52.18 (1.69)	53.55 (3.06)	51.88 (1.39)		46.63 (−3.86)	53.40 (2.91)	51.76 (1.27)		50.49
C ₁₄	27.29 (6.06)	26.21 (4.98)	24.49 (3.26)		22.94 (1.71)	26.00 (4.77)	24.28 (3.05)		21.23
C ₁₅	31.44 (3.02)	32.24 (3.82)	30.73 (2.31)		26.32 (−2.10)	32.25 (3.83)	30.75 (2.33)		28.42
MAE all	5.91	4.41	3.29		6.22	5.60	4.48		
CMAE all	2.53	1.49	1.45		3.63	1.09	0.98		
MAE <i>sp</i> ²	6.87	4.78	3.81		7.89	6.41	5.44		
CMAE <i>sp</i> ²	2.36	1.63	1.52		2.85	1.12	0.94		

From calculations performed in vacuo (in acetonitrile), the isotropic shielding constant of TMS, employed to define the chemical shifts amounts to 193.2, 183.3, 187.3, and 197.4 ppm (193.7, 183.9, 187.8, and 197.9 ppm) at the HF, B3LYP, *m*PW1PW91, and MP2 levels of approximation, respectively. In parentheses are given the δ differences between theory and experiment. MAE and CMAE are provided considering all C atoms or only the *sp*² C atoms

larger, the corrected MAE values reduce to about 1 ppm. These main observations describe well the better agreement sketched in Fig. 2, in particular for the C atoms having δ values larger than 150 ppm. Note again that, from calculations not detailed here, only negligible variations

are obtained when using other, often more extended, basis sets [(aug-)cc-pVDZ and (aug-)cc-pVTZ].

Consequently, the following equations will be used in Sect. 4.4 to estimate the experimental ¹³C chemical shifts from the calculated ones:

$$\delta(\text{Exp, all C}) = -2.98 + 0.9872 \times \delta[\text{B3LYP}/6-311 + \text{G}(2d, p)] \quad (1)$$

$$\delta(\text{Exp, } sp^2 \text{ C}) = -4.15 + 0.9953 \times \delta[\text{B3LYP}/6-311 + \text{G}(2d, p)] \quad (2)$$

$$\delta(\text{Exp, all C}) = -1.74 + 0.9658 \times \delta[\text{B3LYP}/6-311 + \text{G}(2d, p)/\text{IEFPCM}(\text{acetonitrile})] \quad (3)$$

$$\delta(\text{Exp, } sp^2 \text{ C}) = 2.14 + 0.9383 \times \delta[\text{B3LYP}/6-311 + \text{G}(2d, p)/\text{IEFPCM}(\text{acetonitrile})] \quad (4)$$

Table 3 Linear regression parameters for all and for sp^2 C atoms characterizing the relationship between the experimental (in acetonitrile) and theoretical ^{13}C chemical shifts of the coumarin and coumarin-6H for different levels of approximation using the 6-311+G(2d,p) basis set

$\delta(\text{Exp}) = a + b \times \delta(\text{Theor})$	a	b	R
In vacuo			
All C atoms			
HF	-0.61	0.9532	0.9978
B3LYP, Eq. 1	-2.98	0.9872	0.9991
<i>m</i> PW1PW91	-1.36	0.9826	0.9920
sp^2 C atoms			
HF	10.63	0.8743	0.9878
B3LYP, Eq. 2	-4.15	0.9953	0.9927
<i>m</i> PW1PW91	-3.85	1.0003	0.9937
In acetonitrile (PCM)			
All C atoms			
HF	6.75	0.8968	0.9956
B3LYP, Eq. 3	-1.74	0.9658	0.9995
<i>m</i> PW1PW91	-0.16	0.9614	0.9996
sp^2 C atoms			
HF	26.21	0.7614	0.9841
B3LYP, Eq. 4	2.14	0.9383	0.9969
<i>m</i> PW1PW91	2.51	0.9422	0.9973

R is the correlation coefficient

4.3 ^1H chemical shifts

The same approach was adopted for the ^1H chemical shifts. Table 4 lists the ^1H δ for different levels of approximation and compares them to the experimental data recorded in acetonitrile. The confrontation theory–experiment (see also Fig. 3) highlights several trends: (1) in most cases, all methods slightly overestimate the chemical shifts, except for H_2 (and, at a lower extent, H_{12} and H_{13} of coumarin-6H) with the B3LYP and MP2 levels of approximation, (2) all $\Delta\delta = \delta_{\text{exp}} - \delta_{\text{theor}}$ are small, (3) there are, however, inversions between the δ amplitudes for consecutive protons (see H_2 vs. H_6 δ values), and (4) contrary to the ^{13}C δ , the increase of $\Delta\delta$ is almost proportional to the experimental chemical shifts. Improvements in the ^1H chemical shifts were also sought by performing linear regressions with or without distinguishing between the H atoms—or rather the C atoms on which they are attached. Table 5 summarizes these results. Contrary to the ^{13}C case, using DFT, there are little differences when considering all protons or only those attached to sp^2 C atoms: the intercept is small and the slope close to one. Nevertheless, like for ^{13}C , the largest deviations with respect to the linear regression are found for the largest deshieldings. Using the latter fitted parameters, the B3LYP/6-311+G(2d,p) approach leads to corrected MAEs of 0.07 and 0.08 ppm with Eqs. 5 and 6,

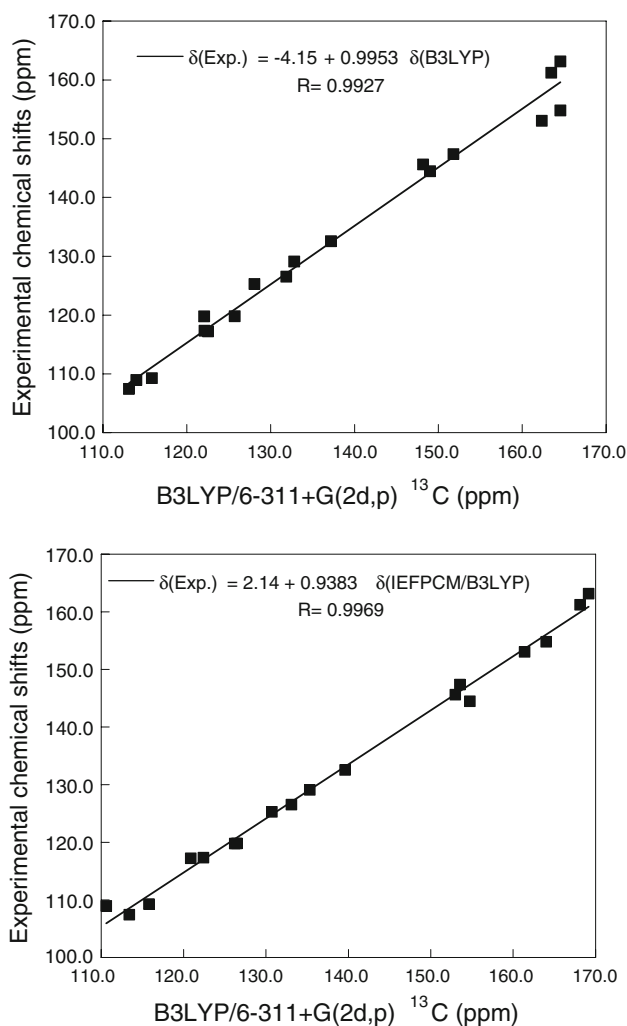


Fig. 2 Relationships between the experimental (in acetonitrile) and B3LYP/6-311+G(2d,p) ^{13}C chemical shifts (in ppm) of coumarin and coumarin-6H for all sp^2 C atoms as determined with (bottom) and without (top) accounting for solvent effects within the PCM scheme

respectively, in comparison with 0.07 and 0.09 ppm without linear regression. The improvement is almost negligible. Using *m*PW1PW91, the CMAE values are similar to the B3LYP ones but the improvement over the MAEs is larger. The MP2 values are not as accurate as the DFT results. By comparing the results on ^{13}C and ^1H , it can also be concluded that different functionals perform best for different nuclei and that these relative performances can be tuned upon using the linear relationship corrections.

When accounting for the solvent effects using the PCM scheme, the CMAE values go down to 0.05 ppm for both B3LYP and *m*PW1PW91 XC functionals (Table 4) while, in the aromatic ^1H δ range, the large chemical shifts ($\delta \sim 8$ ppm) are predicted with similar accuracy to the small ones ($\delta \sim 6$ –7 ppm). This improvement towards better modeling the real systems is however accompanied by larger and positive deviations with respect to

Table 4 Theoretical and experimental ^1H chemical shifts (in ppm) for coumarin and coumarin-6H in acetonitrile

Atoms	Theory, in vacuo				Theory, in acetonitrile (PCM)				Experiment
	HF	B3LYP	<i>m</i> PW1PW91	MP2	HF	B3LYP	<i>m</i> PW1PW91	MP2	
Coumarin									
H ₁	6.32 (−0.05)	6.39 (0.02)	6.46 (0.09)	6.47 (0.10)	6.62 (0.25)	6.73 (0.36)	6.81 (0.44)	7.16 (0.79)	6.37
H ₂	8.05 (0.21)	7.72 (−0.12)	7.79 (−0.05)	7.63 (−0.21)	8.94 (1.10)	8.45 (0.61)	8.54 (0.70)	7.73 (−0.11)	7.84
H ₄	7.84 (0.30)	7.62 (0.08)	7.71 (0.17)	7.61 (0.07)	8.46 (0.92)	8.16 (0.62)	8.27 (0.73)	7.32 (−0.22)	7.54
H ₅	7.42 (0.14)	7.39 (0.11)	7.47 (0.19)	7.58 (0.30)	7.89 (0.61)	7.84 (0.56)	7.94 (0.66)	7.96 (0.68)	7.28
H ₆	8.00 (0.41)	7.74 (0.15)	7.84 (0.25)	7.71 (0.12)	8.47 (0.88)	8.17 (0.58)	8.28 (0.69)	7.90 (0.31)	7.59
H ₇	7.70 (0.39)	7.55 (0.24)	7.62 (0.31)	7.74 (0.43)	7.98 (0.67)	7.85 (0.54)	7.93 (0.62)	8.27 (0.96)	7.31
Coumarin-6H									
H ₁	5.98 (0.11)	5.94 (0.07)	6.00 (0.13)		6.09 (0.22)	6.15 (0.28)	6.23 (0.36)		5.87
H ₂	7.83 (0.28)	7.43 (−0.12)	7.51 (−0.04)		8.76 (1.21)	8.06 (0.51)	8.16 (0.61)		7.55
H ₄	7.34 (0.43)	7.03 (0.12)	7.11 (0.20)		7.97 (1.06)	7.49 (0.58)	7.60 (0.69)		6.91
H ₁₀	2.98 (0.20)	2.98 (0.20)	2.95 (0.17)		2.80 (0.02)	2.94 (0.16)	2.91 (0.13)		2.78
H ₁₁	1.92 (0.01)	1.95 (0.04)	1.91 (0.00)		1.86 (−0.05)	2.00 (0.09)	1.97 (0.06)		1.91
H ₁₂	3.10 (−0.15)	3.23 (−0.02)	3.19 (−0.06)		3.08 (−0.17)	3.39 (0.14)	3.36 (0.11)		3.25
H ₁₃	3.10 (−0.15)	3.23 (−0.02)	3.20 (−0.05)		3.07 (−0.18)	3.38 (0.13)	3.35 (0.10)		3.25
H ₁₄	1.98 (0.07)	1.93 (0.02)	1.88 (−0.03)		1.82 (−0.09)	1.97 (0.06)	1.94 (0.03)		1.91
H ₁₅	2.74 (0.02)	2.81 (0.09)	2.78 (0.06)		2.72 (0.00)	2.90 (0.18)	2.88 (0.16)		2.72
MAE all	0.18	0.07	0.10		0.49	0.37	0.41		
CMAE all	0.11	0.07	0.06		0.17	0.06	0.05		
MAE <i>sp</i> ²	0.26	0.09	0.14		0.79	0.51	0.61		
CMAE <i>sp</i> ²	0.10	0.08	0.08		0.12	0.05	0.05		

From both calculations performed in vacuo and in acetonitrile, the TMS isotropic shielding constant amounts to 32.2, 31.9, 31.8, and 31.8 ppm at the HF, B3LYP, *m*PW1PW91, and MP2 levels of approximation, respectively. In parentheses are given the δ differences between theory and experiment. MAE and CMAE are provided considering all C atoms or only the *sp*² C atoms

experiment. Indeed, for the *sp*² C atoms, the MAE goes from 0.09 (0.14) to 0.51 (0.61) ppm using the B3LYP (*m*PW1PW91) XC functional. This nicely demonstrates a typical compensation of errors. Accounting for solvent effects, large *R* values are associated with slopes of the order of 0.85 and intercepts of 0.6 ppm. Similar conclusions are obtained by employing more extended basis sets. In conclusion, the CMAE values go down to 0.05 ppm, which demonstrates the reliability of the approach.

Consequently, the following equations will be used in Sect. 4.4 to estimate the experimental ^1H chemical shifts from the calculated ones:

4.4 Application to coumarin-343 derivatives

These different linear regressions were then employed to predict the ^{13}C and ^1H chemical shifts of the “*sp*²” atoms of the C343-dea (**3**), C343-crown (**4**), and C343-dibenzo-crown (**5**) compounds (Fig. 1). Therefore, the calculated chemical shifts have been corrected using Eqs. 2 and 4 for ^{13}C and Eqs. 6 and 8 for ^1H , respectively. The comparison between the theoretical and experimental ^{13}C and ^1H NMR chemical shifts is presented in Table 6. No matter which correction equation is used (i.e. distinguishing or not between the *sp*² and *sp*³ atoms, considering or not

$$\delta(\text{Exp, all H}) = -0.04 + 0.9972 \times \delta[\text{B3LYP}/6 - 311 + \text{G}(2d, p)] \quad (5)$$

$$\delta(\text{Exp, H attached to } sp^2 \text{ C}) = -0.05 + 0.9987 \times \delta[\text{B3LYP}/6 - 311 + \text{G}(2d, p)] \quad (6)$$

$$\delta(\text{Exp, all H}) = 0.11 + 0.9174 \times \delta[\text{B3LYP}/6 - 311 + \text{G}(2d, p)] / \text{IEFPCM}(\text{acetonitrile}) \quad (7)$$

$$\delta(\text{Exp, H attached to } sp^2 \text{ C}) = 0.60 + 0.8546 \times \delta[\text{B3LYP}/6 - 311 + \text{G}(2d, p)] / \text{IEFPCM}(\text{acetonitrile}) \quad (8)$$

Table 5 Linear regression parameters for all H atoms and for H atoms attached to sp^2 C atoms characterizing the relationship between the experimental (in acetonitrile) and theoretical ^1H chemical shifts of coumarin and coumarin-6H as a function of the level of approximation using the 6-311+G(2d,p) basis set

$\delta(\text{Exp}) = a + b \times \delta(\text{Theor})$	a	b	R
In vacuo			
All H atoms			
HF	0.17	0.9421	0.9984
B3LYP, Eq. 5	-0.04	0.9972	0.9990
mPW1PW91	0.05	0.9738	0.9990
H atoms attached to sp^2 C atoms			
HF	0.85	0.8521	0.9838
B3LYP, Eq. 6	-0.05	0.9987	0.9828
mPW1PW91	-0.03	0.9857	0.9820
In acetonitrile (PCM)			
All H atoms			
HF	0.54	0.8322	0.9968
B3LYP, Eq. 7	0.11	0.9174	0.9997
mPW1PW91	0.19	0.8961	0.9997
H atoms attached to sp^2 C atoms			
HF	1.95	0.6556	0.9766
B3LYP, Eq. 8	0.60	0.8546	0.9978
mPW1PW91	0.59	0.8455	0.9971

R is the correlation coefficient

explicitly the direct effects of the solvent), theory reproduces most of the features of the experimental spectra, i.e. the chemical shift values and the differences of chemical shifts between consecutive H or C atoms.

Nevertheless, among these chemical shifts, $\delta(^{13}\text{C}_2)$ and $\delta(^1\text{H}_2)$ are difficult to estimate and, for compound **3**, the overestimations remain as large as 5.91 and 0.22 ppm, respectively. To trace the possible origin of these discrepancies, we looked at the δ values of the different conformers. However, they vary little (maximum change of 2.0 and 0.1 ppm for ^{13}C and ^1H , respectively, like in the case of the two conformers of compound **3**) so that the differences found between theory and experiment do not originate from errors in the MB distribution. Moreover, when the conformer energies for compound **3** are calculated at the MP2/6-311G(d) level of approximation, the MAE is only reduced from 1.66 to 1.65 ppm whereas $\delta(^{13}\text{C}_2)$ changes by less than 0.2 ppm. Then, we investigated the effect of modifying the $\theta_{2-1-16-\text{O}}$ angle by a step of 5° around the equilibrium position. Again, the impact is small (148.62 ppm for ^{13}C and 7.77 ppm for ^1H , which still gives an overestimation of 5.79 and 0.21 ppm, respectively) whereas the energy increases, which reduces the weight of these conformations in the MB distribution. We have further checked that these poor estimates are not connected to the fact that the LYP correlation functional lacks equal spin

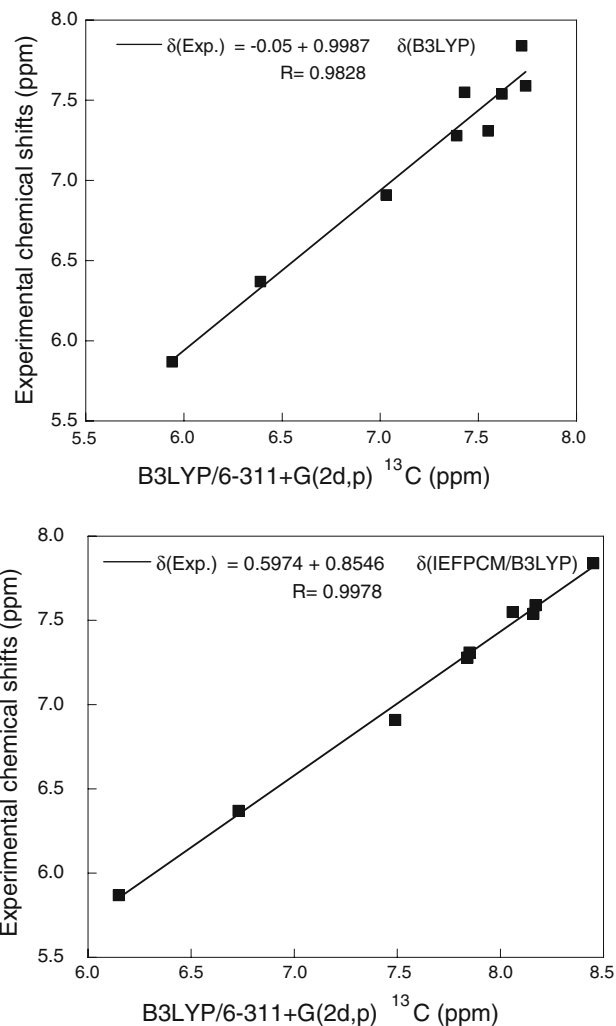


Fig. 3 Relationships between the experimental (in acetonitrile) and B3LYP/6-311+G(2d,p) ^1H chemical shifts (in ppm) of coumarin and coumarin-6H for H atoms attached to sp^2 C atoms with (bottom) and without (top) accounting for solvent effects within the PCM scheme

correlation and exaggerates opposite-spin correlation as discussed by Filatov and Cremer [42]. This was achieved by performing additional IEFPCM(acetonitrile)/B3PW91/6-311+G(2d,p) calculations for C343-dea but no improvement was observed with respect to B3LYP. Thus, the remaining differences come probably from specific interactions with solvent molecules, including possible interactions with water molecules present in acetonitrile. Such large differences between the theoretical and experimental values are also observed for compound **4**, with errors on $\delta(^{13}\text{C}_2)$ and $\delta(^1\text{H}_2)$ of 3.40 and 0.23 ppm, respectively.

Moreover, comparing the results of Table 6 for the different fluoroionophores, the variations of δ when going from the 'In gas phase' to the 'In acetonitrile' columns present similar trends considering the three ligands, except

Table 6 Theoretical (B3LYP/6-311+G(2d,p)) versus experimental ^{13}C and ^1H NMR chemical shifts (in ppm, with respect to TMS) for the characteristic “ sp^2 ” atoms of C343-dea, C343-crown, and C343-dibenzocrown after accounting for linear regression corrections

Atoms	Theory		Experiment
	In gas phase	In acetonitrile (PCM)	
C343-dea			
C ₁	120.12	116.32	119.97
C ₂	149.20	148.74	142.83
C ₃	110.16	109.56	108.22
C ₄	126.73	126.37	126.58
C ₅	118.56	122.06	119.97
C ₆	146.45	147.01	147.60
C ₇	105.89	106.85	106.84
C ₈	156.59	153.20	152.80
C ₉	159.12	158.57	160.37
C ₁₆	167.19	166.05	166.66
MAE	1.77	1.66	
H ₂	8.06	7.78	7.56
H ₄	6.96	6.93	6.96
C343-crown			
C ₁	120.92	117.60	–
C ₂	146.83	147.21	143.81
C ₃	111.70	110.85	108.23
C ₄	127.96	127.46	126.75
C ₅	117.71	121.23	120.19
C ₆	147.11	147.92	147.88
C ₇	107.91	108.99	106.80
C ₈	156.38	153.09	152.92
C ₉	158.71	158.61	160.34
C ₁₆	169.02	167.83	167.91
MAE	2.03	1.33	
H ₂	8.14	7.84	7.61
H ₄	7.33	6.83	6.97
C343-dibenzocrown			
C ₁	119.26	115.64	
C ₂	149.40	149.05	
C ₃	111.90	111.39	
C ₄	128.84	128.58	
C ₅	117.79	121.07	
C ₆	148.29	148.75	
C ₇	108.26	108.85	
C ₈	157.45	154.03	
C ₉	158.40	158.12	
C ₁₆	169.65	168.05	
MAE	–	–	
H ₂	8.24	7.95	7.61 ^a
H ₄	7.17	7.13	6.81 ^a

^a In CDCl₃

for the case of C₂ of C343-crown. In such a case, a small increase is predicted instead of a small decrease obtained with the other two ligands. This difference has been attributed to the changes in the MB distribution of the different conformers of C343-crown upon taking into account the effects of the solvent (see Sect. 4.1) in combination with their slightly different chemical shifts. This has further been substantiated by comparing the chemical shifts of similar conformations for the three fluoroionophores, i.e. conformer ‘b’ of C343-dea with conformer ‘c’ of C343-crown (see Table 1). In this case, $\delta(^{13}\text{C}_2)$ of C343-dea and C343-crown amount to 148.28 and 148.75 ppm when the initial calculations do not account for the effects of the solvent whereas after including these within the PCM scheme, the $\delta(^{13}\text{C}_2)$ values are 147.73 and 148.44 ppm, respectively.

5 Conclusions and outlook

^1H and ^{13}C NMR chemical shifts of coumarin derivatives have been determined using first principles approaches with and without accounting for the effects of the solvent. First, the calculated values for coumarin and coumarin-6H have been compared to experiment in order to assess their reliability. Good linear relationships are obtained between theory and experiment, which allows correcting the calculated values for systematic errors. This is particularly the case when accounting for the effects of the solvent at the PCM level because the δ values larger than 150 ppm have been shown to be more difficult to reproduce. Using DFT and hybrid XC functionals (B3LYP and *m*PW1PW91), the final accuracy of the method, estimated from the CMAE values, amounts to about 1 ppm for ^{13}C and 0.05 ppm for ^1H . This calibration step extends our recent works dealing with the chemical shifts of PVC chains and models [7, 10, 43, 44] to aromatic compounds. Though these corrections might appear scientifically unsatisfactory, these are particularly useful for addressing problems of chemical interest. Then, in order to illustrate the reliability of the approach, the NMR signatures of coumarin-343 derivatives have been evaluated using these linear correction schemes. With the exception of the atoms in position 2 of the aromatic ring, good agreement with experiment is achieved.

Acknowledgments This work is dedicated to Prof. S. Suhai, a leading scientist in the field of polymer electronic structure calculations. This work was supported from research grants from the Belgian Government (IUAP No P06-27 “Functional Supramolecular Systems”). Ph. d’A. is grateful to the Fonds pour la Formation à la Recherche dans l’Industrie et dans l’Agriculture (FRIA) for his PhD grant. E.B. thanks the IUAP program No P06-27 for her postdoctoral

grants. B.C. thanks the Belgian National Fund for Scientific Research for his Research Director position and L.M. for her research fellow position. The calculations were performed on the Interuniversity Scientific Computing Facility (ISCF), installed at the Facultés Universitaires Notre-Dame de la Paix (Namur, Belgium), for which the authors gratefully acknowledge the financial support of the FNRS-FRFC, and the “Loterie Nationale” for the convention no 2.4.617.07.F, and of the FUNDP.

References

1. Helgaker T, Jaszunski M, Ruud K (1999) *Chem Rev* 99:293
2. Gauss J, Stanton JF (2002) *Adv Chem Phys* 123:355
3. Kaupp M, Bühl M, Malkin VG (eds) (2004) *Calculation of NMR and EPR parameters*. Wiley-VCH, Weinheim
4. Bagno A, Rastrelli F, Saielli G (2006) *Chem Eur J* 12:5514
5. Bifulco G, Dambruoso P, Gomez-Paloma L, Riccio R (2007) *Chem Rev* 107:3744
6. Ando I, Kuroki S, Kurosu H, Yamanobe T (2001) *Prog NMR Spectrosc* 39:79
7. d'Antuono Ph, Botek E, Champagne B, Wieme J, Reyniers M-F, Marin GB, Adriaensens PJ, Gelan JM (2007) *Chem Phys Lett* 436:388
8. Chesnut DB (1996) The ab initio computation of nuclear magnetic resonance chemical shielding. In: Lipkowitz KB, Boyd DB (eds) *Reviews in computational chemistry*, vol 8. VCH, Weinheim, p 245
9. Rablen PR, Pearlman SA, Finkbiner J (1999) *J Phys Chem A* 103:7357
10. d'Antuono Ph, Botek E, Champagne B, Spassova M, Denkova P (2006) *J Chem Phys* 125:144309
11. Bifulco G, Gomez-Paloma L, Riccio R (2003) *Tetrahedron Lett* 44:7137
12. Trabelsi M, Salem M, Champagne B (2003) *Org Biomol Chem* 1:3839
13. Poater J, van Lenthe E, Baerends EJ (2003) *J Chem Phys* 118:8584
14. Allen MJ, Keal TW, Tozer DJ (2003) *Chem Phys Lett* 380:380
15. Tähtinen P, Bagno A, Klika KD, Pihlaja K (2003) *J Am Chem Soc* 125:4609
16. Hieringer W, Della Sala F, Görling A (2004) *Chem Phys Lett* 383:115
17. Arbuznikov AV, Kaupp M (2004) *Chem Phys Lett* 386:8
18. Gryffter-Keller A, Molchanov S (2004) *Mol Phys* 102:1903
19. Wiitala KW, Hoye TR, Cramer CJ (2006) *J Chem Theor Comput* 2:1085
20. Wiitala KW, Al-Rashid ZF, Dvornikovs V, Hoye TR, Cramer CJ (2007) *J Phys Org Chem* 20:345
21. Wiitala KW, Cramer CJ, Hoye TR (2007) *Magn Reson Chem* 45:819
22. Rychnovsky SD (2006) *Org Lett* 8:2895
23. Bagno A, Rastrelli F, Saielli G (2007) *J Org Chem* 72:7373
24. Pennanen TS, Lantto P, Sillanpää AJ, Vaara J (2007) *J Phys Chem A* 111:182
25. Bassarello C, Bifulco G, Montoro P, Skhirtladze A, Kemertelidze E, Pizzi C, Piacente S (2007) *Tetrahedron* 63:148
26. Baldrige KK, Siegel JS (2008) *Theor Chem Acc* 120:95
27. Habib-Jiwan J-L, Branger C, Soumillon J-Ph, Valeur B (1998) *J Photochem Photobiol A Chem* 116:127
28. Leray I, Habib-Jiwan J-L, Branger C, Soumillon JPh, Valeur B (2000) *J Photochem Photobiol A Chem* 135:163
29. Taziaux D, Soumillon J-Ph, Habib-Jiwan J-L (2004) *J Photochem Photobiol A Chem* 162:599
30. Maton L, Taziaux D, Soumillon J-Ph, Habib Jiwan J-L (2005) *J Mater Chem* 15:2928
31. Löhr HG, Vögtle F (1985) *Acc Chem Res* 18:65
32. Valeur B (2001) *Molecular fluorescence: principles and applications*. Wiley-VCH Verlag GmbH, Weinheim
33. Fedorova OA, Fedorov YV, Vedernikov AI, Gromov SP, Yescheulova OV, Alifimov MV, Woerner M, Bossmann S, Braun A, Saltiel J (2002) *J Phys Chem A* 106:6213
34. Korolev VV, Vorobyev DYu, Glebov EM, Grivin VP, Plyusnin VF, Koshkin AV, Fedorova OA, Gromov SP, Alifimov MV, Shklyaev YV, Vshivkova TS, Rozhkova YS, Tolstikov AG, Lokshin VV, Samat A (2007) *J Photochem Photobiol A Chem* 192:75
35. Berthet J, Mischeau JC, Lokshin V, Vales M, Vermeersch G, Delbaere S (2008) *Org Lett* 10:3773
36. Ditchfield R (1971) *J Am Chem Soc* 93:5287
37. Wolinski K, Hilton JF, Pulay P (1990) *J Am Chem Soc* 112:8251
38. Cammi R, Mennucci B, Tomasi J (1999) *J Chem Phys* 110:7627
39. Manalo MN, de Dios AC, Cammi R (2000) *J Phys Chem A* 104:9600
40. Tomasi J, Mennucci B, Cammi R (2005) *Chem Rev* 105:2999
41. Frisch MJ, Trucks GW, Schlegel HB, Scuseria GE, Robb MA, Cheeseman JR, Montgomery JA Jr, Vreven T, Kudin KN, Burant JC, Millam JM, Iyengar SS, Tomasi J, Barone V, Mennucci B, Cossi M, Scalmani G, Rega N, Petersson GA, Nakatsuji H, Hada M, Ehara M, Toyota K, Fukuda R, Hasegawa J, Ishida M, Nakajima T, Honda Y, Kitao O, Nakai H, Klene M, Li X, Knox JE, Hratchian HP, Cross JB, Adamo C, Jaramillo J, Gomperts R, Stratmann RE, Yazyev O, Austin AJ, Cammi R, Pomelli C, Ochterski JW, Ayala PY, Morokuma K, Voth GA, Salvador P, Dannenberg JJ, Zakrzewski VG, Dapprich S, Daniels AD, Strain MC, Farkas O, Malick DK, Rabuck AD, Raghavachari K, Foresman JB, Ortiz JV, Cui Q, Baboul AG, Clifford S, Cioslowski J, Stefanov BB, Liu G, Liashenko A, Piskorz P, Komaromi I, Martin RL, Fox DJ, Keith T, Al-Laham MA, Peng CY, Nanayakkara A, Challacombe M, Gill PMW, Johnson B, Chen W, Wong MW, Gonzalez C, Pople JA (2004) *GAUSSIAN 03, Revision C.02*. Gaussian, Inc., Wallingford
42. Filatov M, Cremer D (2005) *J Chem Phys* 123:124101
43. d'Antuono Ph, Botek E, Champagne B, Wieme J, Reyniers M-F, Marin GB, Adriaensens PJ, Gelan JM (2005) *Chem Phys Lett* 211:207
44. d'Antuono Ph, Botek E, Champagne B, Wieme J, Reyniers M-F, Marin GB, Adriaensens PJ, Gelan JM (2008) *J Phys Chem B* 112:14804